

Effects of Jet Flow Pulsation on Diffusion Flame Performance

A.M. Moustafa, M.M.Kamal, Ashraf M. Hamed, Ahmed E Hussin

Abstract: The objective of the current research is the experimental investigation of the pulsating flow effects on the combustion performance in terms of the flame temperature distribution, the heat transfer rate, the combustion efficiency and the exhaust gas analysis. The flow pulsation provided through a rotary ball valve in accordance with a variable speed motor arrangement increased the flame temperature fluctuation and the magnitude of heat release. The flow pulsation provides a highly turbulent flame wherein the vortices are enlarged. Increasing Strouhal number [St] of the LPG fuel and air flow increases the time-averaged flame temperature of the pulsating flame up to a saturation level that is dictated by the heat transfer rate enhancement. The maximum average flame temperature is 1263°C at $St=0.041$, $r=0$ mm and 100 mm from the burner inlet. In addition, increasing the pulsating flow amplitude increases the convection and radiation heat fluxes from the pulsating flame. While increasing the pulsation decreases the exhaust UHC due to increasing the turbulent kinetic energy across the pulsating flame, the exhaust NO_x slightly increases due to increasing the heat release rate and the flame temperatures. Pulsation thus enhances the combustion efficiency inside the industrial combustors.

Keywords: External pulsation, pulsating flame, Inlet flame port, Diffusion flame, Pulsation frequency, pulsator combustor.

I. INTRODUCTION

Pulsating flames acquire the features of turbulent combustion which is industrially attractive. In this respect, the pulsation process enhances the combustion performance in terms of the combustion efficiency and heat transfer. Some research works were devoted to measure the flame temperature fluctuations, while other experimental tests were carried out to quantify the heat transfer characteristics for turbulent confined flames (with and without pulsation). The effect of the pulsation frequency, Reynolds number and the firing rate on Nusselt number in cases of upstream and downstream pulsation effects was experimentally investigated. A ball valve that is driven by a variable speed motor provides a flexible mechanism of pulsation. The pulsating flow improves the convection heat transfer rate inside the combustor. Increasing the pulsation frequency and Reynolds number increases the average heat transfer coefficient [1-9]. At the pulsation frequency of 3.3 Hz, the maximum enhancement was obtained where the heat transfer coefficient increased by 17.68 and 44.4%, respectively in the

upstream and downstream regions. Upon increasing the firing rate, the enhancement in the mean Nusselt number is more prominent in case of the flame downstream regions. The experimental results on forced convection heat transfer showed that the values of Nusselt number increase upon increasing Reynolds number for both pulsating and non-pulsating flows in the range of Reynolds number, Re between 100 and 2000. It was found that Nusselt number for laminar pulsating flow decreases by an average value of about 22% below what corresponds to the non-pulsating flow when the pulsation amplitude was increased. An empirical formula was derived for Nusselt number as a function of Reynolds number and the pulsation amplitude. Additional experiments were stated to be still necessary for the other flow regimes, pulsating frequencies and flow configurations to explore whether the heat transfer rates increase or decrease upon introducing the pulsating flow effects [10-15].

The vortex shedding and the corresponding heat transfer around a cylinder in a cross flow with free-stream pulsations was studied experimentally in the range of Strouhal number, $St=0-1.76$ and relative amplitude from 0 to 0.85. While the free-stream velocity followed a nearly harmonic law, the flow visualization analysis of the cylinder wake zone classified the flow patterns around the cylinder into four main groups in which the large-scale vortices behave differently as a function of the dimensionless frequency, St , and the relative amplitude of pulsation. It was revealed that depending on the free-stream pulsation amplitude, different flow patterns can occur at a fixed Strouhal number. This is dependent on a new dimensionless number which was introduced as the ratio of the inertial force due to the flow acceleration in its global unsteady motion to the inertial force due to the streamline curvature around the cylinder. It was demonstrated that the heat transfer from the cylinder in the cross-flow could be enhanced by forced flow pulsations. The heat transfer enhancement by the pulsating cross-flow was testified by two symmetric vortices that were shown to be shed from the opposite sides of the cylinder during each period of pulsation. Flow visualization was performed at the blockage ratio of 0.29 and 0.13, where the corresponding aspect ratios were respectively 3.45 and 7.6. More results are required to fully represent all flow structures and modes of heat transfer [16-24]. It is noted that in the previous studies, the pulsating flow effect characteristics of the diffusion flame have not been fully addressed. Therefore, the objective of the present research is to experimentally investigate the effect of Strouhal number of flow pulsation (via the spinning of a ball valve) on the performance of the diffusion flame. The flame temperature fluctuations are recorded at the non-pulsating flame condition ($St=0$) and the pulsating flame conditions (at different Strouhal number values including $St=0.005, 0.026, 0.041, 0.056, 0.066$).

Revised Manuscript Received on November 30, 2020.

A.M. Moustafa, Professor, Department of Mechanical Power, Ain Shams University, Egypt.

M.M.Kamal, Assistant Professors, Faculty of Engineering, Ain Shams University, Egypt.

Ashraf M. Hamed, Assistant Professors, Faculty of Engineering, Ain Shams University, Egypt.

Ahmed E Hussin, Assistant Professors, Faculty of Engineering, Ain Shams University, Egypt.

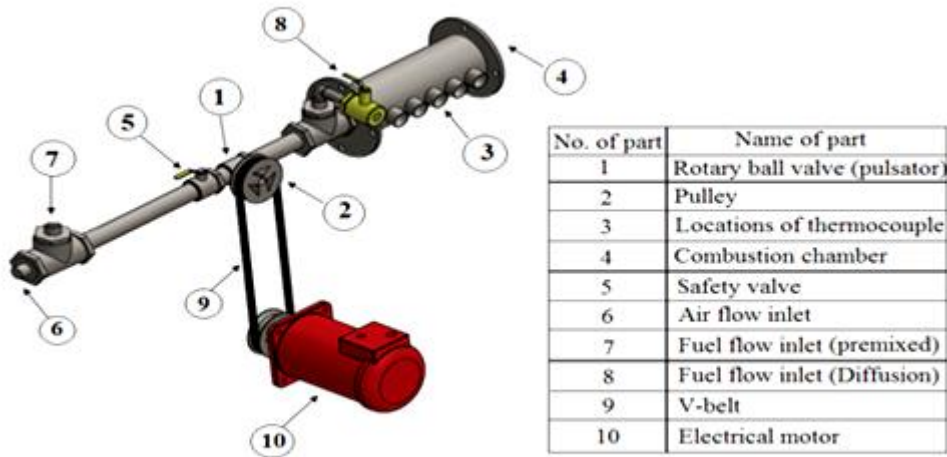


Fig.1.a. Test rig and layout of pulsating combustion system

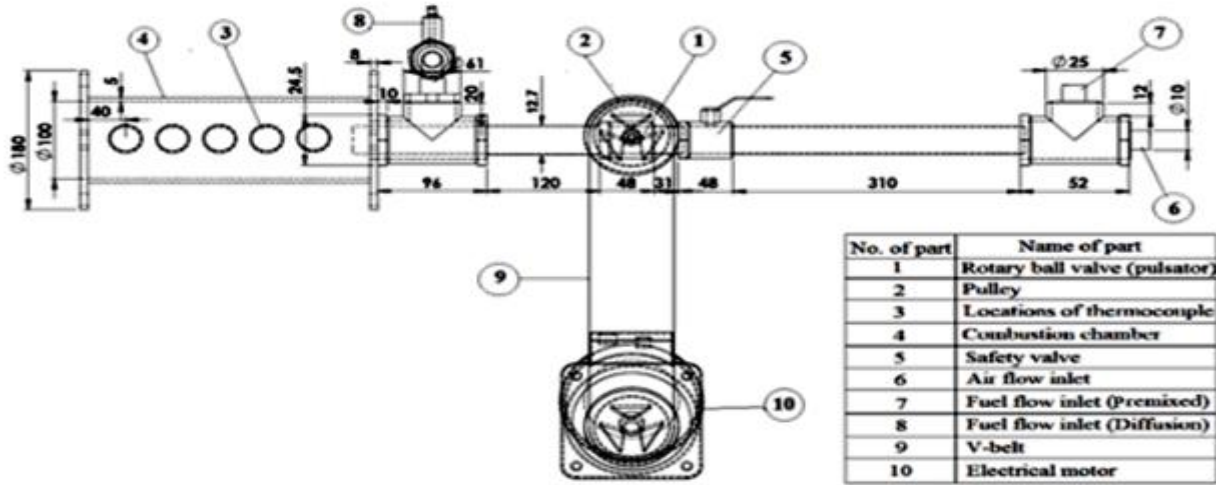


Fig.1.b. Test rig section

II. TEST RIG AND EXPERIMENTAL WORK

The construction details of the test rig employed to investigate the combustion pulsating system via rotary ball valve (pulsator) are shown in the following figure, (see Fig. 1.a-b). From Figs.1.a-b, it can be noted that pulsating process of the flow is completed through a pulley and rotary valve (pulsator) which rotate via the DC motor by V-belt. By using of the inverter, speed of the pulsating flow has been changed via the DC motor and thus there is different Strouhal number of the pulsating flow. The mixture flow of fuel (LPG) and oxidizer enters the combustion chamber through diameter nozzle tip equals 12.25 mm in partially premixed case while the air flows through inner diameter nozzle tip equals 12.25 mm and fuel flows through outer diameter equals 21 mm. The flow rate of fuel and air has been measured by using four rotameters.

The S-type thermocouple (Platinum/Rhodium (90%Pt, 10%Rh)), which has diameter probe equals 0.25 mm, it has been used to measure flame temperature fluctuation, instantaneously. Max 31856 module and an Arduino Uno card have been used via an Arduino circuit to display temperatures data on the computer screen.

III. RESULTS AND DISCUSSION

In the current research, by using S-Type thermocouple, Arduino Uno circuit and Arduino program, the time-averaged flame temperature has been measured at different longitudinal distances ($x=40, 70, 100$ burner inlet. At each value of $[x]$, the temperature is measured at, 130 and 160 mm) from the different radii ($r=0, 10, 20, 30$ and 40 mm). The measurement procedure is completed at different values of Strouhal number ($St=0, 0.005, 0.026, 0.041, 0.056$ and 0.066) when the overall excess air is 20% and the burner inlet diameter is 12.7 mm. The analysis of the results is shown as follows:

A. Effect of Different Strouhal Number on the Flame Temperature

In this part, the time-averaged flame temperature has been determined at five planes and each plane has five radii. The effect of different Strouhal number will be shown as follows;



1. Effect of Strouhal Number on the Flame Temperatures in Longitudinal Direction

In this part, there is distribution of the time averaged flame temperature at five planes and each plane have five radii and at different strouhal number; this will be show as follows;

Time- Averaged Flame Temperatures Distributions at 40 mm from the Burner Inlet

The variation of the time-averaged flame temperatures with Strouhal number is recorded at $x=40$ mm from the burner inlet for the radial positions, $r=0, 10, 20, 30$ and 40 mm receptivity from center of the combustion chamber, this is shown in Fig. 2.

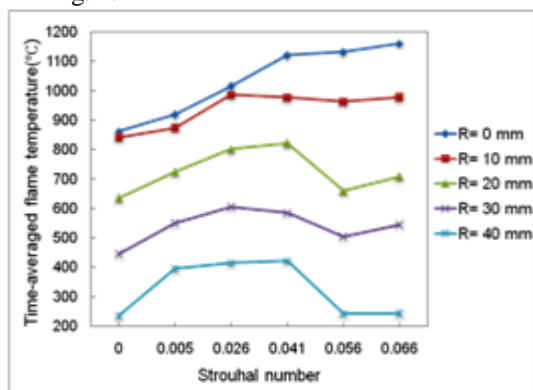


Figure 2: Distribution of the time-averaged flame temperatures at $x=40$ mm

From Fig.2, in general, an increasing strouhal number of the pulsating flow (fuel) increases the time averaged flame temperature due to the pulsation generates shearing phenomena between the flame layers. This shearing produces vortices and eddies of the flame and turbulent flame and thus increasing the time average flame temperature.

From the previous figure, the time average flame temperature exists inside center of the flame is larger than the time averaged flame temperature at surface of the flame beside the wall of the combustor. For example, at center of the flame and strouhal number equals zero, the time averaged flame temperature equals 862.45°C . The rate of heat transfer at center of the flame is low, on the other hand, at surface of the flame and strouhal number equals zero, and the time averaged flame temperature equals 235.11°C . The rate of heat transfer at surface of the flame beside the wall of the combustor is high. Fig.3 reflects the overall trend of the time averaged flame temperatures at different strouhal number. As increasing strouhal number increases the time averaged flame temperature. [25]

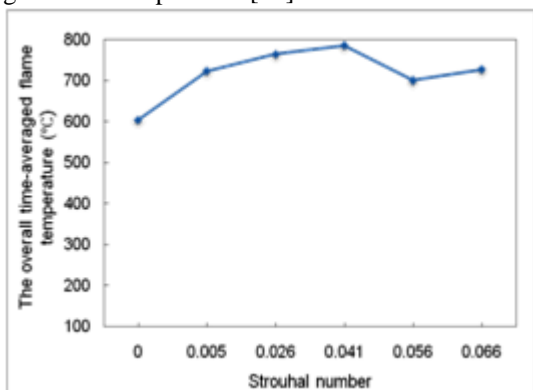


Figure 3: Variation of the overall average of time-averaged temperatures at $x=40$ mm

Time- Averaged Flame Temperatures Distributions at 70 mm from the Burner Inlet

The variation of the time-averaged flame temperatures with Strouhal number is recorded at $x=70$ mm from the burner inlet for the radial positions, $r=0, 10, 20, 30$ and 40 mm receptivity from center of the combustion chamber, this is shown in Fig. 4.

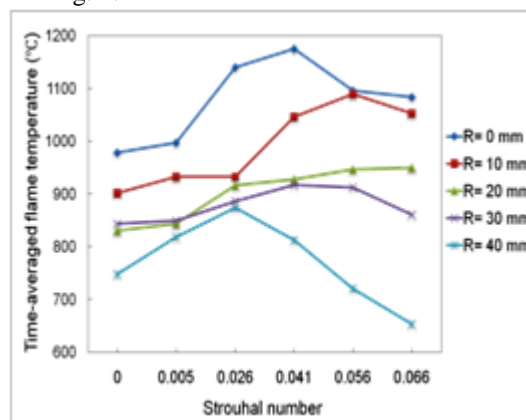


Figure 4: Distribution of the time-averaged flame temperatures at $x=70$ mm

From Fig.4, the same as the previous plane, an increasing strouhal number of the pulsating flow (fuel) increases the time averaged flame temperature. At the most planes, the time averaged flame temperatures decrease at $St=0.051$ and 0.066 due to exist of large eddies and thus low of flame density. The time averaged flame temperatures at the present plane are higher than the time averaged flame temperatures at the previous plane due to increasing shearing rate in this region at the present plane. Fig.5 reflects the overall trend of the time averaged flame temperatures at different strouhal number. Also, at this plane the time averaged flame temperature increases by increasing strouhal number directly. At the current plane, the overall average time averaged flame temperatures are higher than like it at the previous plane.

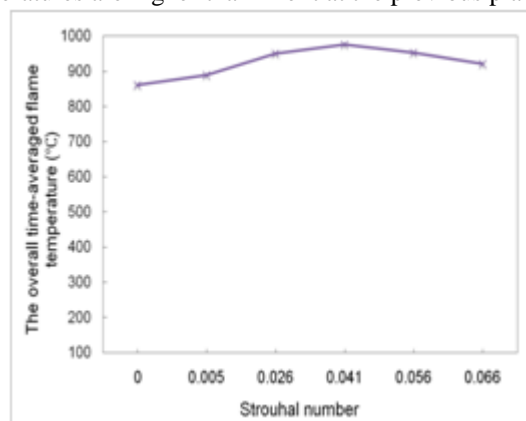


Figure 5: Variation of the overall average of time-averaged temperatures at $x=70$ mm

Time- Averaged Flame Temperatures Distributions at 100 mm from the Burner Inlet

The variation of the time-averaged flame temperatures with Strouhal number is recorded at $x=100$ mm from the burner inlet for the radial positions, $r=0, 10, 20, 30$ and 40 mm receptivity from center of the combustion chamber, this is shown in Fig. 6.



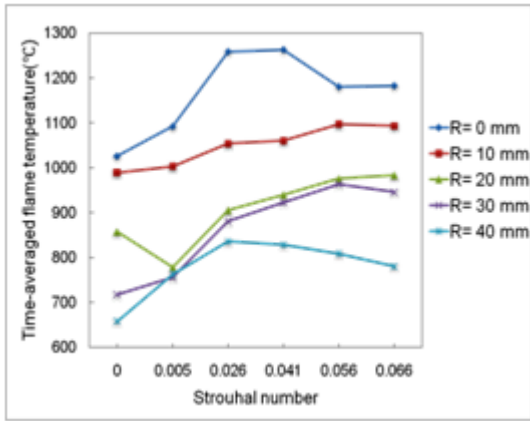


Figure 6: Distribution of the time-averaged flame temperatures at x=100 mm

From Fig.6, also, an increasing strouhal number of the pulsating flow (fuel) increases the time averaged flame temperature at the current plane. The time averaged flame temperatures at the present plane are higher than the time averaged flame temperatures at the two previous planes due to increasing shearing rate in this region. Fig.7 reflects the overall trend of the time averaged flame temperatures at different strouhal number. In addition to the overall average time averaged flame temperatures are higher than like it at the previous planes.

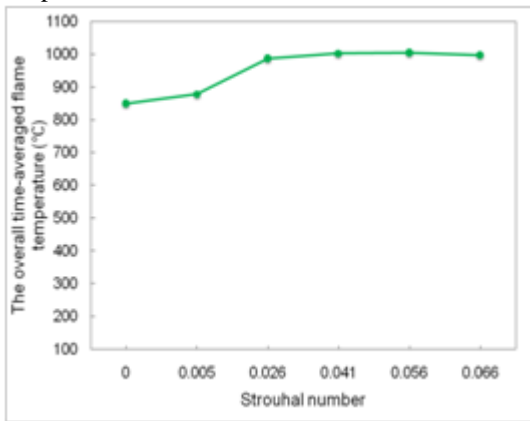


Figure 7: Variation of the overall average of time-averaged temperatures at x=100 mm

Time- Averaged Flame Temperatures Distributions at 130 mm from the Burner Inlet

The variation of the time-averaged flame temperatures with Strouhal number is recorded at x= 130 mm from the burner inlet for the radial positions, r=0, 10, 20, 30 and 40 mm receptivity from center of the combustion chamber, this is shown in Fig. 8.

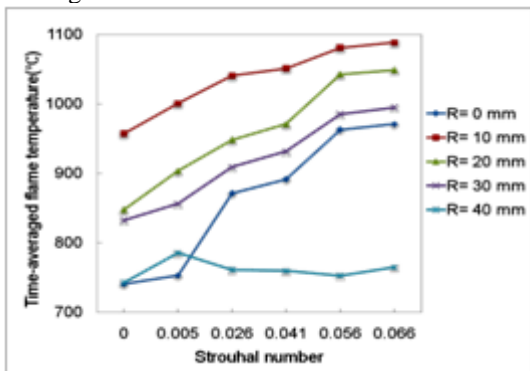


Figure 8: Distribution of the time-averaged flame temperatures at x=130 mm

From Fig.8, like as the previous planes, in general, an increasing strouhal number of the pulsating flow (fuel) increases the time averaged flame temperature. The time averaged flame temperatures at center of the flame are lower than like it at R= 10, 20 and 30 mm due to exist of an integral scale which has the large eddies in a turbulent flow; that eddies with low density and thus lowertemperature.

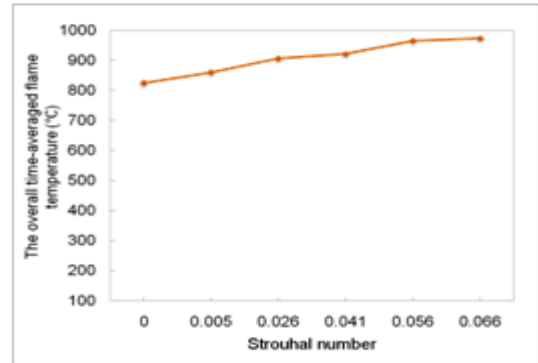


Figure 9: Variation of the overall average of time-averaged temperatures at x=130 mm

From Fig.9, the overall time averaged flame temperature increases directly by increasing strouhal number. The overall average of time averaged flame temperatures are lower than like it at the previous plane, due to decreasing velocity of the layers.

Time- Averaged Flame Temperatures Distributions at 160 mm from the Burner Inlet

The variation of the time-averaged flame temperatures with Strouhal number is recorded at x= 160 mm from the burner inlet for the radial positions, r=0, 10, 20, 30 and 40 mm receptivity from center of the combustion chamber. This is shown in Fig. 10.

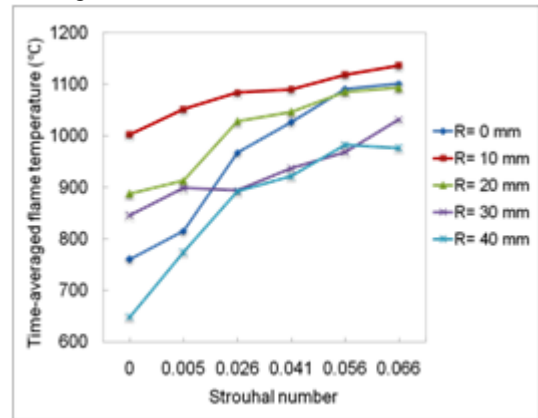


Figure 10: Distribution of the time-averaged flame temperatures at x=160 mm

Also, from Fig.10, like as the previous planes, in general, an increasing strouhal number of the pulsating flow (fuel) increases the time averaged flame temperature. The time averaged flame temperatures at center of the flame are lower than like it at R= 10 and 20 mm due to exist of an integral scale which has the large eddies in a turbulent flow; as low density and thus lowertemperature.

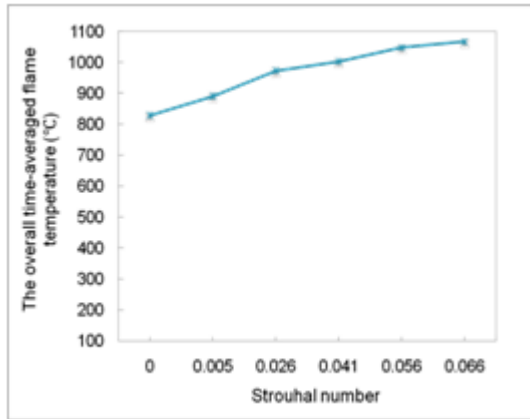


Figure 11: Variation of the overall average of time-averaged temperatures at x=160 mm

From Fig.11, the overall time averaged flame temperature increases directly by increasing strouhal number. Here, the overall average of time averaged flame temperatures are higher than like it at the previous plane. This is due to exist of Kolmogorov micro-scale that is the smallest eddies in turbulent flow with high density turbulent flame more than like it at the previous plane.

2. Effect of the Pulsating Flow on the Overall Average of the Time-Averaged Flame Temperatures

It is interesting to note the effect of Strouhal number on the maximum value of the overall average temperature. Such peak occurs at St=0.041, radius(R) = 0 mm and plane (Pl) =10 mm.

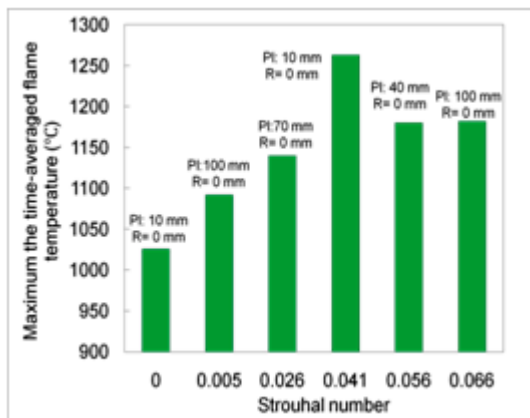


Figure 11: Distribution of the maximum time- averaged flame temperatures inner the combustion chamber

3. Effect of Strouhal Number on the Flame Temperatures in Radial Direction

The distribution of the average flame temperatures at five planes of the combustion chamber as x= 40, 70, 100, 130 and 160 mm receptively from the burner inlet will be show as follows;

Time-Averaged Flame Temperature Distribution at r=0 mm

In addition, the time- averaged flame temperature will be illustrated in the following figure;

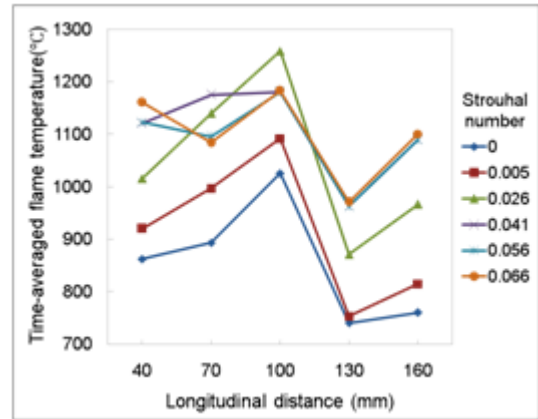


Figure 12: Distribution of the time-averaged flame temperatures at r= 0 mm

It is clear from Fig. 12 that increasing the pulsation frequency enhances the heat release and increases the time-averaged flame temperature and additionally displaces the peak temperature upward, thus reducing the flame length (at r=0). Increasing strouhal number decreases the Kolmogorov length scale at which the higher dissipation rate of the turbulent kinetic energy increases the rates of reaction at the molecular level.

Time-Averaged Flame Temperatures Distribution at r=10 mm

The time- averaged flame temperatures will be illustrated in the following figure;

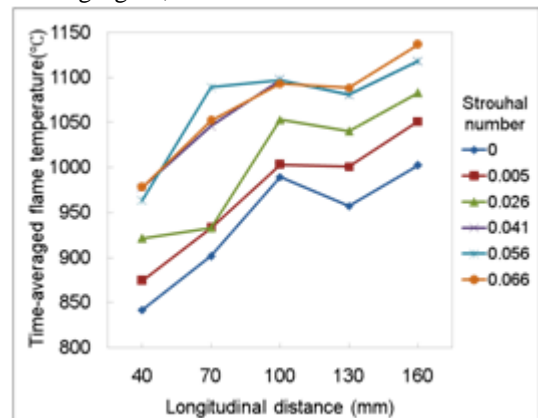


Figure 13: Distribution of the time-averaged flame temperatures at r= 10 mm

From Fig. 13, also, increasing strouhal number increases shearing rate between flame layers and more heat releases and thus more the time averaged flame temperatures. The pulsation increases eddies and vortices and thus the flame length reduce. The time averaged flame temperatures at the present radius are lower than like it at the previous radius as convection heat transfer increases because of the high shearing rates in the vicinity of the combustor wall, thus reducing the thermal boundary layer thickness.

On the other hand, radiation heat transfer increases because of the enlargement in the heat release rates.

Time-Averaged Flame Temperatures Distribution at r=20 mm

The time- averaged flame temperatures will be illustrated in the following figure;

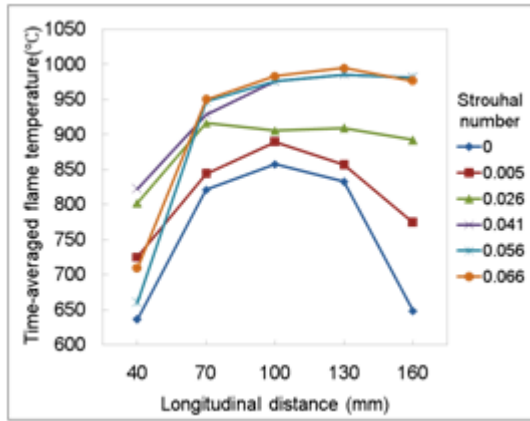


Figure 14: Distribution of the time-averaged flame temperatures at r= 20 mm

From Fig. 14, the same as the previous plane, increasing Strouhal number increases shearing rate between flame layers and more heat releases and thus more the time averaged flame temperatures. It increases eddies and vortices and thus the flame length reduce. Also, the time averaged flame temperatures at the present radius are lower than like it at the previous radius as convection rates increases in radial direction.

Time-Averaged Flame Temperatures Distribution at r=30 mm

The time- averaged flame temperatures will be illustrated in the following figure;

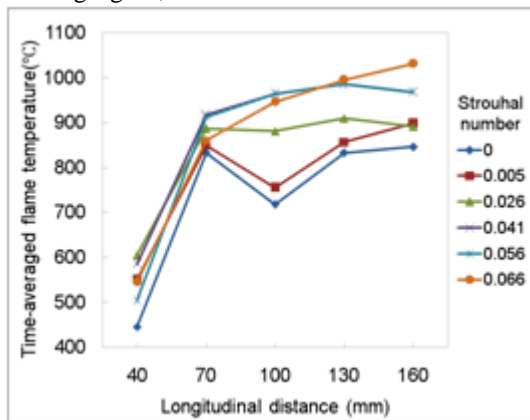


Figure 15: Distribution of the time-averaged flame temperatures at r= 30 mm

From Fig. 15, in addition, the same as the previous plane, increasing Strouhal number increases shearing rate between flame layers and more heat releases and thus more the time averaged flame temperatures. The pulsation increases eddies and vortices and thus the flame length reduce. Also, the time averaged flame temperatures at the present radius are lower than like it at the previous radius as convection rates increases in radial direction.

Time-Averaged Flame Temperatures Distribution at r=40 mm

The time- averaged flame temperatures will be illustrated in the following figure;

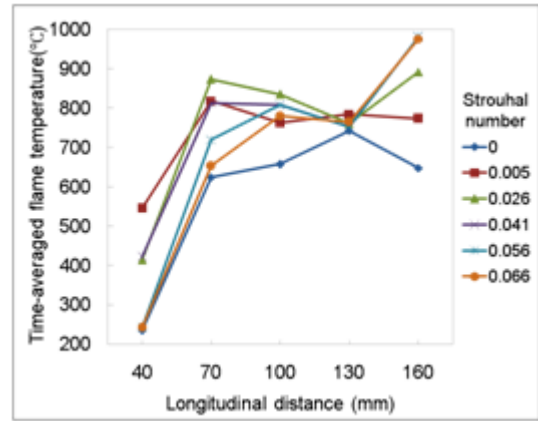


Figure 16: Distribution of the time-averaged flame temperatures at r= 40 mm

From Fig. 16, the same as the previous plane, increasing Strouhal number increases shearing rate between flame layers and more heat releases and thus more the time averaged flame temperatures. The pulsation increases eddies and vortices and thus the flame length reduce. Also, the time averaged flame temperatures at the present radius are lower than like it at the previous radius as convection rates increases in radial direction.

4. Effect of the Pulsating Flow on the Flame Convection and Radiation Heat Transfer Rates

Here, it is noted that the relation between convection, radiation and total heat and different Strouhal number inside the combustion chamber; this will be shown in the following figure;

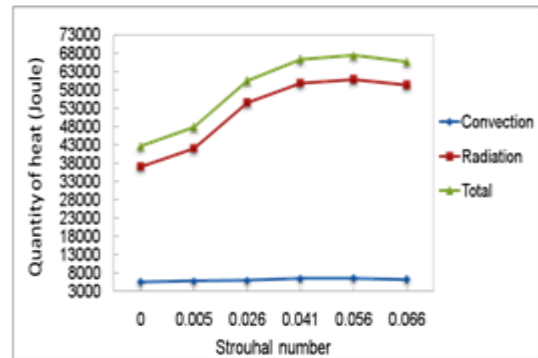


Figure 17: Variation of the convection, radiation and total heat transfer rates with strouhal number

As noticed from Fig. 17, the convection heat transfer rate increases with Strouhal number since the temperature gradients within the combustor wall thermal boundary layer become steeper upon increasing the pulsation frequency. As the vortices are thus enlarged, the resultant corrugations enlarge the inner diffusion flame and consequently the radiation heat transfer rate from the inner reaction zone increases. Furthermore, the increase in the heat release rates yields higher rates of radiation from the outer non-premixed flame. It follows that the total rate of heat transfer increases with Strouhal number.

IV. EXHAUST GAS ANALYSIS

In this the part, there is gases analysis which emitted from the flame such as; UHC and NO_x, this will be shown in the following figure;

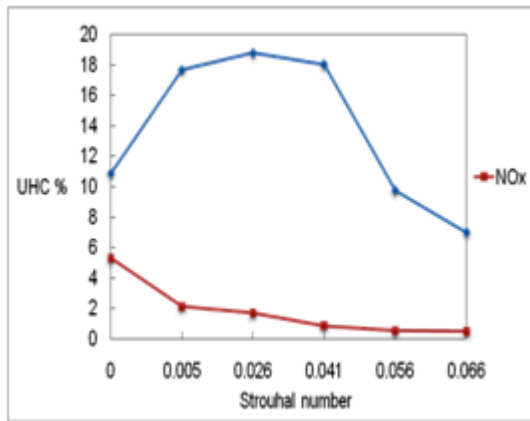


Figure 18: Variation of the UHC and NOx Concentrations with Strouhal number

Figure 18 shows that the UHC exhaust concentration decreases due to pulsation which improves the mixing between the excess fuel and the co-flowing air.

On the other hand, the exhaust NO_x (mg/mm³) concentration first increases when the mixing and combustion rates become enhanced such that the consequent increase in the temperatures across the reaction zone yields higher rates of NO_x formation via the thermal route. By the further increase in Strouhal number, the resultant higher heat transfer rates and the corresponding higher levels of uniformity within the flame eddies decrease the peak flame temperature and thus reduce the NO_x exhaust concentrations.

5. Effect of the Pulsating Flow on the Combustion Efficiency

In this the part, the efficiency of combustion has been calculated from the following equation; $\eta_{\text{combustion}} = 1 - \text{UHC}\%$ and effect of the pulsating flow on different strouhal number, this will be shown in the following figure;

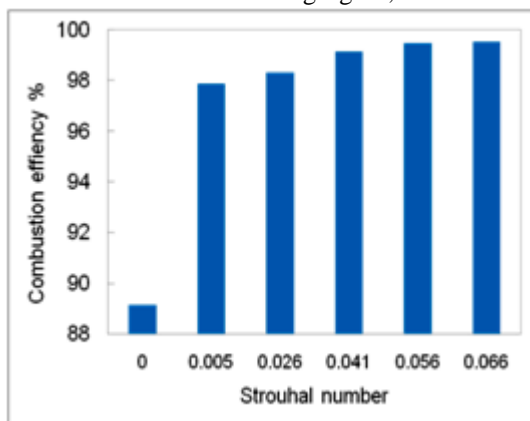


Figure 19: Variation of the Combustion efficiency with Strouhal number

From Fig. 19, it is noted that the maximum combustion efficiency is 99.52%. Increasing the flow pulsation frequency increases the combustion efficiency since the turbulence intensity increases, thus increasing the mixing and reaction rates towards more complete combustion.

V. CONCLUSIONS

The obtained results showed that:

- Pulsation of the flow mixture (fuel LPG and air) generates eddies and vortices and thus turbulent flame occurred in diffusion flame case.
- Increasing the pulsating flow frequency increases the convection and radiation heat transfer rates from the

flame via increasing the eddy transport and the turbulent kinetic energy cascade.

- Increasing Strouhal number of the pulsating flow shrinks the pulsating flame length.
- Increasing the flow pulsation frequency increases the combustion efficiency since the turbulence intensity increases.

REFERENCES

1. Plavnik, Z.Z., Severyanin, V.S., Matta, L.M. and Feingold, V.L., 2001. Pulse combustion system and method. U.S. Patent 6,210,149.
2. Plavnik, G., 2006, May. Pulse combustion technology. In 14th Annual North American Waste-to-Energy Conference (pp. 143-148). American Society of Mechanical Engineers Digital Collection.
3. Keller, J.O. and Hongo, I., 1990. Pulse combustion: The mechanisms of NO_x production. *Combustion and Flame*, 80(3-4), pp.219-237.
4. Poppe, C., Sivasegaram, S. and Whitelaw, J.H., 1998. Control of NO_x emissions in confined flames by oscillations. *Combustion and Flame*, 113(1-2), pp.13-26.
5. Dec, J.E. and Keller, J.O., 1989. Pulse combustor tail-pipe heat-transfer dependence on frequency, amplitude, and mean flow rate.
6. Boulanger, J., 2010. Laminar round jet diffusion flame buoyant instabilities: Study on the disappearance of varicose structures at ultra-low Froude number. *Combustion and flame*, 157(4), pp.757-768.
7. Biswas, K., Zheng, Y., Kim, C.H. and Gore, J., 2007. Stochastic time series analysis of pulsating buoyant pool fires. *Proceedings of the Combustion Institute*, 31(2), pp.2581-2588.
8. Kartheekyan, S. and Chakravarthy, S.R., 2006. An experimental investigation of an acoustically excited laminar premixed flame. *Combustion and flame*, 146(3), pp.513-529.
9. Fujisawa, N., Abe, T., Yamagata, T. and Tomidokoro, H., 2014. Flickering characteristics and temperature field of premixed methane/air flame under the influence of co-flow. *Energy conversion and management*, 78, pp.374-385.
10. Kartheekyan, S. and Chakravarthy, S.R., 2006. An experimental investigation of an acoustically excited laminar premixed flame. *Combustion and flame*, 146(3), pp.513-529.
11. Berg, I.A., Khudyakov, P.Y. and Oschepkova, V.Y., 2016. Automation of analytic complex for the investigation of pulsating combustion. *Fundamental research*, 6, pp.24-28.
12. Berg, I.A., Porshnev, S.V., Oschepkova, V.Y. and Medvedev, A.N., 2017, June. Frequency-domain analysis for pulsating combustion of gaseous fuel. In *AIP Conference Proceedings* (Vol. 1836, No. 1, p. 020036). AIP Publishing LLC.
13. Sawarkar, P., Sundararajan, T. and Srinivasan, K., 2017. Effects of externally applied pulsations on LPG flames at low and high fuel flow rates. *Applied Thermal Engineering*, 111, pp.1664-1673.
14. Nicoli, C., Haldenwang, P. and Suard, S., 2005. Analysis of pulsating spray flames propagating in lean two-phase mixtures with unity Lewis number. *Combustion and flame*, 143(3), pp.299-312.
15. Hamins, A., Yang, J.C. and Kashiwagi, T., 1992, January. An experimental investigation of the pulsation frequency of flames. In *Symposium (international) on combustion* (Vol. 24, No. 1, pp. 1695-1702). Elsevier.
16. Yilmaz, H., Cam, O. and Yilmaz, I., 2020. Experimental investigation of flame instability in a premixed combustor. *Fuel*, 262, p.116594.
17. Coats, C.M., Chang, Z. and Williams, P.D., 2010. Excitation of thermoacoustic oscillations by small premixed flames. *Combustion and flame*, 157(6), pp.1037-1051.
18. Yang, F. and Kong, W., 2015. Pulsating instability in H₂-air partially premixed flames. *Proceedings of the Combustion Institute*, 35(1), pp.1057-1064.
19. McQuay, M.Q., Dubey, R.K. and Carvalho Jr, J.A., 2000. The effect of acoustic mode on time-resolved temperature measurements in a Rijke-tube pulse combustor. *Fuel*, 79(13), pp.1645-1655.
20. Kilcarslan, A., 2005. Frequency evaluation of a gas-fired pulse combustor. *International journal of energy research*, 29(5), pp.439-454.
21. Saitoh, T. and Otsuka, Y., 1976. Unsteady behavior of diffusion flames and premixed flames for counter flow geometry. *Combustion Science and Technology*, 12(4-6), pp.135-146.
22. Searby, G., 1992. Acoustic instability in premixed flames. *Combustion science and technology*, 81(4-6), pp.221-23.

Effects of Jet Flow Pulsation on Diffusion Flame Performance

23. Wang, Q., Huang, H.W., Tang, H.J., Zhu, M. and Zhang, Y., 2013. Nonlinear response of buoyant diffusion flame under acoustic excitation. *Fuel*, 103, pp.364-372.
24. Balachandran, R., Ayoola, B.O., Kaminski, C.F., Dowling, A.P. and Mastorakos, E., 2005. Experimental investigation of the nonlinear response of turbulent premixed flames to imposed inlet velocity oscillations. *Combustion and Flame*, 143(1-2), pp.37-55.
25. McQuay, M.Q., Dubey, R.K. and Carvalho Jr, J.A., 2000. The effect of acoustic mode on time-resolved temperature measurements in a Rijke-tube pulse combustor. *Fuel*, 79(13), pp.1645-1655

AUTHORS PROFILE



Ahmed Mohamed Moustafa borned in Cairo, Egypt. Ahmed graduated from the Faculty of Engineering, Ain Shams University in 2009, Cairo, Egypt, He studied in Mechanical Engineering department. He concerns with combustion Engineering and internal combustion engine.



Mohmoud Mohamed Kamal borned in Cairo, Egypt. Mahmoud graduated from the Faculty of Engineering, Ain shams University in 1998, Cairo, Egypt. He studied in Mechanical power engineering department. He is current a Lecturer at the department of Mechanical Power Engineering since 2005. He concerns with combustion engineering, internal combustion engine, thermo fluid, heat transfer, fluid mechanics, and turbo machine.



Ashraf Mostafa Hamed borned in Cairo, Egypt. Ashraf graduated from the Faculty of Engineering, Ain shams University in 2003. He is current a Lecturer at the department of Mechanical Power Engineering since 2013. He concerns with Turbomachinery, Wind Energy, Fluid Dynamics, Combustion and Computational Fluid Dynamics.



Ahmed Mohamed Hussein borned in Cairo, Egypt. Ahmed from the Faculty of Engineering, Ain shams University in 2000. He is current a Lecturer at the department of Mechanical Power Engineering since 2012. He concerns with Fluid Mechanics, Computational Fluid Dynamics, Engineering Thermodynamics, Turbulence, Energy Engineering, Heat Exchangers, Experimental Fluid Mechanics, Applied Thermodynamics, Heat Transfer, Convection.